Sensors and Materials, Vol. 18, No. 4 (2006) 173–181
MYU Tokyo

S & M 0641

Langasite Membranes for Surface Acoustic Wave Pressure Sensors

Tao Han*, Xiaojun Ji and Wenkang Shi

Department of Instrumentation Engineering, Shanghai Jiaotong University,
1954 Huashan Road, Shanghai 200030

(Received February 2, 2005; accepted August 26, 2005)

Key words: surface acoustic wave, pressure sensor, langasite

On the basis of the electroelastic perturbation model, which includes electrical perturbation items, a doubly rotated cut area of langasite (LGS) defined by the Euler angles ϕ, from 137° to 160°, and ψ, from 18° to 25°, is proposed as a design for pressure sensors because it has good temperature stability (TCD < 10 ppm), high electromechanical coupling coefficients ($k^2 > 0.4\%$) and relatively high pressure sensitivity ($6–8 \times 10^{-12}/(Pa \cdot (R/h)^2)$). Differential surface acoustic wave resonators made of LGS (0°, 150° and 22°) have been fabricated and tested. The measured fractional frequency changes among the differential resonators vs pressure from 0 to 0.6 MPa verify that the experimental relative sensitivity is 3.7×10^{-10} fractional frequency change per Pa, which is in agreement with the calculated prediction. The temperature dependence is within 2.5 kHz/°C in the range from 20°C to 100°C.

1. Introduction

Surface acoustic wave (SAW) pressure sensors are passive (no power required), wireless and well suited for measuring pressure in moving objects (e.g., rotating cars and truck tires, hermetically sealed chambers). Quartz is commonly used as a SAW pressure diaphragm.(1–3) It is found that an ST-cut quartz membrane with a SAW propagation direction of 50° with respect to the X-axis has simultaneously both high pressure sensitivity and temperature stability.(1)

Recently, some crystals belonging to the trigonal symmetry group 32, such as $GaPO_4$ and $La_3Ga_5SiO_{14}$ (langasite, LGS), have been utilized as sensors, especially for high temperature applications, because they possess temperature-compensated orientations and strong electromechanical coupling coefficients k^2.(4,5) Without experimental verification, the LGS substrate with Euler angles (0, 30°–50° and 20°–40°) was reported to be useful simultaneously as both SAW pressure and temperature sensors.(6) However, the temperature sensitivity is at least 10 times higher than the pressure sensitivity; thus, substrates with these Euler angles are not suitable for accurate pressure measurement over a wide range of temperatures. In § 3 and 4 of this paper, using both numerical and experimental techniques,

*Corresponding author, e-mail address: than@sjtu.edu.cn

we propose temperature-stable piezoelectric substrates with both high electromechanical coupling coefficients and high pressure sensitivity.

Generally, the first-order perturbation integral by Tiersten and Sinha[7,8] is used as a model of pressure sensitive cuts for SAW in queartz where only the nonlinear elastic constants induced by pressure biasing are not taken into consideration.[1,3,6,9] However, because the k^2 of LGS is 2–3 times higher than quartz, the effective piezoelectric and dielectric constants dependent on the pressure biasing deserve attention. Therefore, we first summarize the electroelastic perturbation model, which includes the electrical perturbation items in § 2.

2. The Piezoelectric Perturbation Model

For the sake of simplification and comparison, we use the symbol convention in Tiersten's paper.[8] The piezoeletric equations for small fields superposed on a pressure bias take the form

$$\tilde{K}_{\mathrm{L}\gamma,\mathrm{L}} = \rho_0 \ddot{u}_\gamma , \tilde{\Delta}_{\mathrm{L,L}} = 0, \tag{1}$$

in which ρ_0 is the mass density and $\ddot{u}_\gamma$ is the second-order differentiation with respect to time of the mechanical displacement from the intermediate coordinate. The relationship between the Piola-Kirchhoff stress tensor $\tilde{K}_{\mathrm{L}\gamma}$, the electric displacement vector $\tilde{\Delta}_{\mathrm{L}}$, the mechanical displacement u_α and the electrical potential $\tilde{\varphi}$ are given by the following constitutive equation

$$\tilde{K}_{\mathrm{L}\gamma} = (c_{\mathrm{L}\gamma\mathrm{M}\alpha} + \hat{c}_{\mathrm{L}\gamma\mathrm{M}\alpha})u_{\alpha,\mathrm{M}} + (e_{\mathrm{ML}\gamma} + \hat{e}_{\mathrm{ML}\gamma})\tilde{\varphi}_{,\mathrm{M}}$$

$$\tilde{\Delta} = (e_{\mathrm{ML}\gamma} + \hat{e}_{\mathrm{ML}\gamma})u_{\alpha,\mathrm{M}} + (\varepsilon_{\mathrm{ML}\gamma} + \hat{\varepsilon}_{\mathrm{ML}\gamma})\tilde{\varphi}_{,\mathrm{M}} . \tag{2}$$

In (2), $c_{\mathrm{L}\gamma\mathrm{M}\alpha}$, $e_{\mathrm{ML}\alpha}$ and $\varepsilon_{\mathrm{LM}}$ denote the second-order elastic, piezoelectric and dielectric constants, respectively. The terms $\hat{c}_{\mathrm{L}\gamma\mathrm{M}\alpha}$, $\hat{e}_{\mathrm{ML}\alpha}$ and $\hat{\varepsilon}_{\mathrm{LM}}$ are the effective elastic, piezoelectric, and dielectric constants dependent on pressure biasing which may be expressed as follows:

$$\hat{c}_{\mathrm{L}\gamma\mathrm{M}\alpha} = T_{\mathrm{LM}}\delta_{\gamma\alpha} + c_{\mathrm{L}\gamma\mathrm{M}\alpha\mathrm{AB}}\overline{E}_{\mathrm{AB}} + c_{\mathrm{LKM}\alpha}w_{\gamma,\mathrm{k}} + c_{\mathrm{L}\gamma\mathrm{KM}}w_{\alpha,\mathrm{k}} - e_{\mathrm{AL}\gamma\mathrm{M}\alpha}\overline{W}_{\mathrm{A}}$$

$$\hat{e}_{\mathrm{M}\alpha} = e_{\mathrm{ML}\alpha\mathrm{BC}}\overline{E}_{\mathrm{BC}} + e_{\mathrm{MLK}}w_{\alpha,\mathrm{K}} + b_{\mathrm{AML}\alpha}\overline{W}_{\mathrm{A}}$$

$$\hat{\varepsilon}_{\mathrm{LM}} = b_{\mathrm{LMCD}}\overline{E}_{\mathrm{CD}} + \varepsilon_{\mathrm{LMC}}\overline{W}_{\mathrm{C}} - 2\varepsilon_0\overline{J}\cdot\overline{E}_{\mathrm{LM}}, \tag{3}$$

where c_{KLMPQ}, $\varepsilon_{\mathrm{KLM}}$ and b_{KLM} denote the third-order elastic, piezoelectric, dielectric and electrostrictive constants, respectively, and TLM, $\overline{E}_{\mathrm{LM}}$, $\overline{W}_{\mathrm{L}}$ and $w_{\gamma,\mathrm{k}}$ denote the components of free space and $\delta_{\gamma\alpha}$ is a Kronecker delta.

According to perturbation theory, the time dependent change in the resonant frequency of SAW devices has the form

$$\frac{\Delta f}{f_0} = \frac{H_{\mathrm{m}}}{2\omega_{\mathrm{m}}^2}. \tag{4}$$

In eq. (4), ω_{m} is the mth eigenfrequency. Considering the traction-free and zero normal component of the electric displacement boundary conditions in the presence of the biasing, H_{m} takes the form

$$H_{\mathrm{m}} = -\int_{\mathrm{V}_0}\left[\hat{c}_{\mathrm{L}\gamma\mathrm{M}\alpha} g^{\mathrm{m}}_{\alpha,\mathrm{M}} g^{\mathrm{m}^*}_{\gamma,\mathrm{L}} + 2\hat{e}_{\mathrm{ML}\gamma} \tilde{f}^{\mathrm{m}}_{,\mathrm{M}} g^{\mathrm{m}^*}_{\gamma,\mathrm{L}} - \hat{\varepsilon}_{\mathrm{LM}} \tilde{f}^{\mathrm{m}}_{,\mathrm{M}} \tilde{f}^{\mathrm{m}^*}_{,\mathrm{L}}\right] dV_0, \tag{5}$$

where * represents a conjugation operator. The terms g_γ and $\tilde{f}$ denote the mth orthonormal eigensolutions of u_γ^{m} and $\tilde{\varphi}^{\mathrm{m}}$ in the presence of biasing, respectively.

$$g_\gamma^m = \frac{u_\gamma^m}{\sqrt{\int_{V_0} \rho_0 u_\gamma^m u_\gamma^{m*} dV}}, \quad \tilde{f}^m = \frac{\tilde{\varphi}^m}{\sqrt{\int_{V_0} \rho_0 u_\gamma^m u_\gamma^{m*} dV}} \tag{6}$$

As shown in Fig.1, a circular piezoelectric membrane of radius R and thickness h with a rigidly fixed periphery is subject to uniform pressure P on one of its surfaces. The static strain tensor components on the membrane can be obtained by using the finite element method (FEM).[(9)]

The normalized pressure sensitivity (NPS) of SAW resonators is defined as:

$$\mathrm{NPS} = \frac{u_\gamma^{\mathrm{m}}}{P \cdot (R/h)^2} \frac{\Delta f}{f_0}, \tag{7}$$

where $\Delta f / f_0$ represents the relative frequency changes resulting from the uniform pressure P. To suppress the temperature dependence of the SAW resonators, the differential configuration between the maximum and the minimum of NPS is defined as DNPS.

3. Predicted Results

We first calculate the theoretical pressure sensitivity of quartz, which is listed in Table 1. Comparing these values with ref. (1), our results are more consistent with the experimental data.

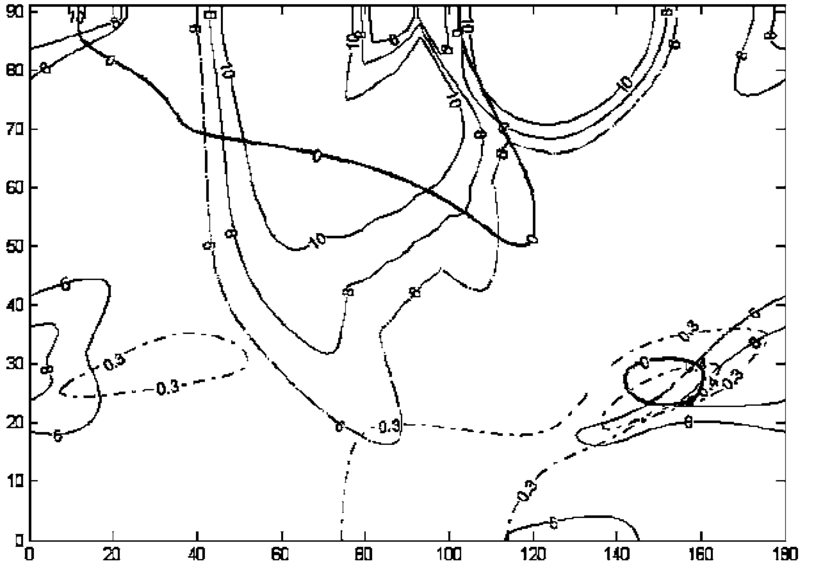

Fig. 1. Contours of DNPS of SAW resonators, TCD and k^2 .

DNPS
TCD
k^2

Table 1

Comparison of results in ref. (1) with numerical results in this paper.

Substrate and orientation	Y-cut quartz	ST-X quartz	ST-X quartz
Thickness, mm	2	2	1.1
Diameter, mm	9	9	12
Distance between resonator centers, nm	4	4	4.8
Resonator center frequency, MHz	310	310	360
Experimental sensitivity (1/Pa) $\times 10^{-12}$	60	20.2	90
Theoretical sensitivity in ref. (1) (1/Pa) $\times 10^{-12}$	75.4	24	100
Calculated theoretical sensitivity in this paper	62.9	20.3	96.6

With the material constants for LGS given in ref. (4), the contours of NPS, the temperature coefficient of delay (TCF), and k^2 as a function of Euler cut angles ϕ of LGS and SAW propagation direction angles ψ are shown in Fig. 1. The optimal doubly rotated cuts for pressure membranes at room temperature are defined by the following intervals of Euler angles: ϕ from 137° to 160° and ψ from 18° to 25°, which exhibit good temperature stability (TCD<10 ppm), high electromechanical coupling coefficients (k^2>0.4%) and relatively high DNPS (about 6–8 × $10^{-12}/(Pa\cdot(R/h)^2)$.

4. Device Fabrication and Measurement Results

To verify the above theoretical results, LGS (0°,150° and 22°) is chosen as the pressure membrane. The TCF, k^2 and DNPS of this substrate are 2.5 ppm at 20°C (0 ppm at 56°C), 0.41% and 7.8 × $10^{-12}/(Pa\cdot(R/h)^2)$, respectively.

According to the pressure sensitivity (Hz/KPa) distribution (Fig. 2) of the substrate under maximum pressure (1 MPa), we determine the radius (R = 7.5 mm) and thickness (h = 1 mm) of circular membranes and the location of dual configuration SAW resonators. One of the two-port SAW resonators (SAWR1) is optimally placed in the center of the LGS circular membrane, where the pressure sensitivity reaches a maximum value of *NPS*. The other resonator (SAWR2) is placed directly above SAWR1 at a distance of 0.78 R (see Fig. 3) to obtain the minimum possible NPS and to reduce temperature influences. Each resonator includes interdigital transducers (IDT) having 56.5 pairs of fingers, a 1200 microns aperture, a 3 microns finger width, and a 50% metallization ratio. The dimensions of each resonator are 7.2 ×1.5 mm². A thin film of Au of 1000 Å thickness is utilized as electrode material because of additional applications at high temperature.

With the package shown in Fig. 4, the sensor is subjected to external pressure using a standard piston oil pressure meter. The S-parameter measurements were taken using the Agilent E5070B vector network analyzer. The frequency response of the SAWR1 resona-

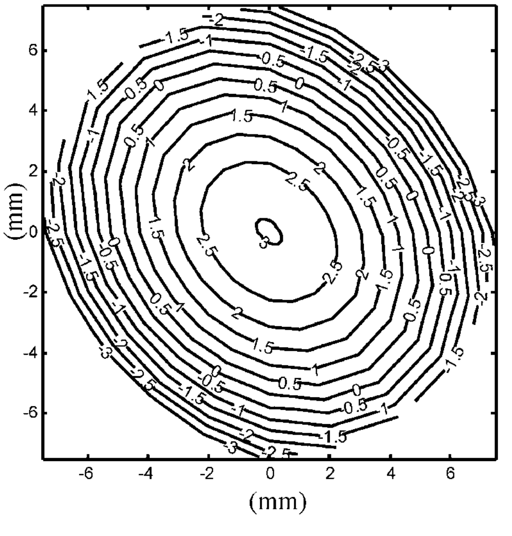

Fig. 2. Map of pressure sensitivity distribution on substrate (0°, 150° and 22°).

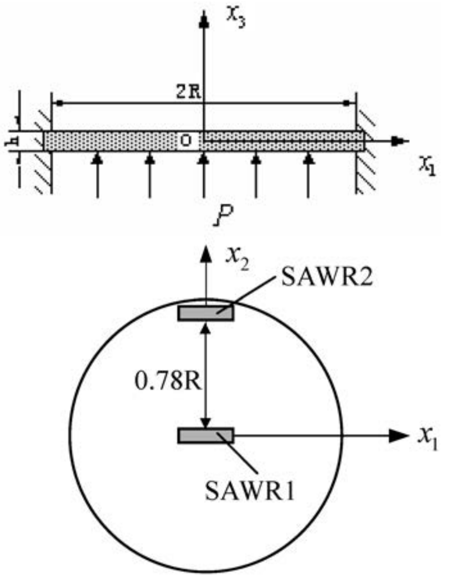

Fig. 3. Cross section of SAW membrane under pressure and location of dual SAW resonators.

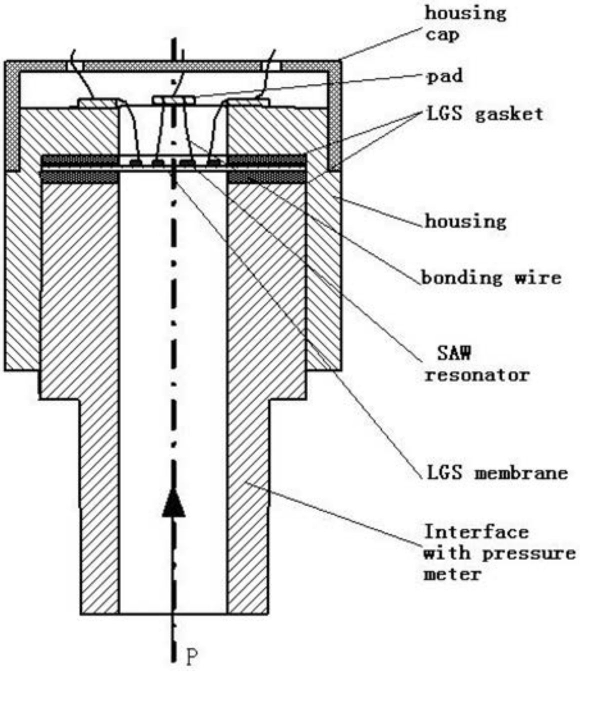

Fig. 4. Diagram of SAW pressure sensor package.

tor is given in Fig. 5. The quality factor is reduced from 2060 to 1620 when the applied pressure ranges from 0 MPa to 0.6 MPa.

Figure 6 displays the dependence on applied pressure of the predicted and measured fractional frequency changes between SAWR1 and SAWR2. The experimental relative sensitivity is 3.7×10^{-10} fractional frequency change per Pa and is in excellent agreement with the theoretical value.

At a pressure of 0.3 MPa, the environmental temperature is varied from 20°C to 100°C using ESPEC test chambers. In Fig. 7, the measured fractional frequency change of SAWR1 is higher than the theoretical value because of the nonlinear coupling between the external applied pressure and temperature. The differential frequency change between SAWR1 and SAWR2 shows temperature dependence because the turnover temperature of LGS is a function of the applied pressure. However, the temperature dependence is within 2.5 kHz/°C in the range from 20°C to 100°C and is almost negligible.

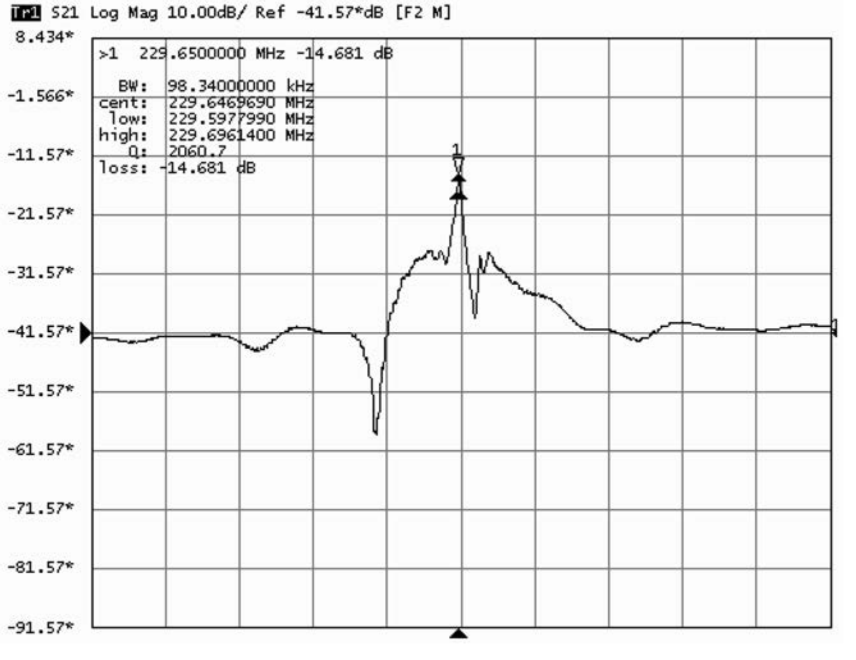

Fig. 5. Frequency response of the center resonator.

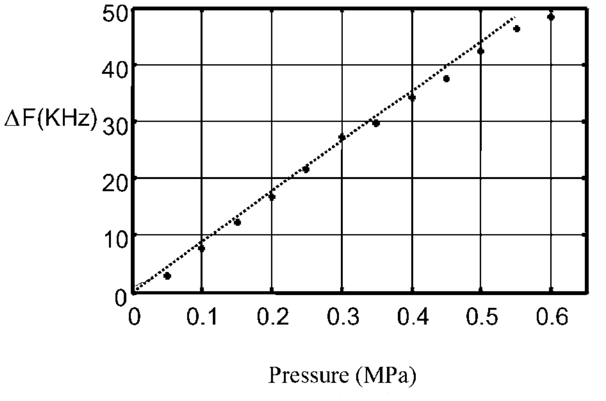

Fig. 6. Predicted and measured fractional frequency change between center resonator and edge resonator when applied pressure is changed from 0 to 0.6 MPa.
• measured
— — — — predicted

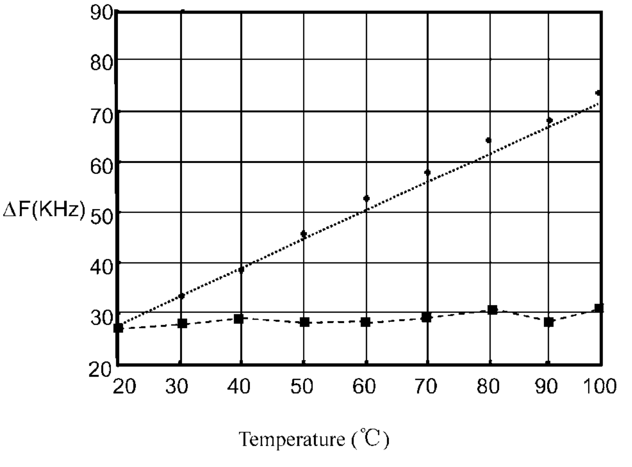

Fig. 7. Predicted and measured fractional frequency change between center resonator and edge resonator
• Measured fractional frequency change of center resonator in range from 20°C to 100°C.
— — Predicted fractional frequency change of center resonator in range from 20°C to 100°C.
▯¡ Measured results of differential frequency output between center resonator and edge resonator in range from 20°C to 100°C.

5. Conclusions

We have experimentally established that a doubly rotated cut area of langasite (LGS) defined by the Euler angles ϕ, from 137° to 160°, and ψ, from 18° to 25°, is suitable for pressure sensors with high electromechanical coupling coefficients and low temperature dependence.

Acknowledgements

Financial support from the Natural Science Foundation of China under grants No. 60274062 and No. 10304012 is gratefully acknowledged. The authors also thank Dr. S. Ballandras of LPMO CNRS Besancon France for help on SAW theoretical analysis, and we also extend our gratitude to Mr. Cao Liang and Mr. Zhu Yong from the Institute of Piezoelectric and Acoustooptic Technology of the Information Industry Ministry (in Chongqing, China) for the fabrication of the SAW devices.

References

1 R. M. Taziev, E. A. Kolosovsky and A. S. Kozlov: IEEE Trans. Ultrason. Ferroelect. Freq. Contr. **42** (1995) 845.
2 W. Buff, S. Klett, M. Rusko, J. Ehrenpfordt and M. Goroll: IEEE Trans. Ultrason. Ferroelect. Freq. Contr. **45** (1998) 1388.
3 M. Jungwrith, H. Scherr and R. Weigel: Acta Mechanica. **158** (2002) 227.
4 A. Bungo, C. Y. Jian and K. Yamaguchi: IEEE Ultrasonics Symp. (1999) 231.
5 N. Naumenko and L. Solie: IEEE Trans. Ultrason. Ferroelect. Freq. Contr. **48** (2001) 530.
6 R. M. Taziev: IEEE International Frequency control symposium and PDA Exhibition (2001) 227
7 B. K. Sinha and W. J. Tanski: J. Appl. Phys. **57** (1985) 767.
8 H. F. Tiersten: J. Acoust. Soc. Am. **64** (1978) 832.
9 S. Ballandras and E. Bigler: IEEE Trans. Ultrason. Ferroelect. Freq. Contr. **45** (1998) 567.